Journal of Applied Sciences

ISSN 1812-5654

science alert

ANSInet
an open access publisher
http://ansinet.com

Journal of Applied Sciences 8 (8): 1479-1486, 2008
ISSN 1812-5654

Three-Dimensional Solutions for Contact Area in Laminated Composite Pinned Joints with Symmetric and Non-Symmetric Stacking Sequences

[1]H. Javadi, [1]I. Rajabi, [2]V. Yavari and [2]M.H. Kadivar
[1]Air Naval Research Center, Shiraz, Iran
[2]Department of Mechanical Engineering, Shiraz University, Shiraz, Iran

Abstract: The aim of this study is computing and evaluating the behavior of the laminated composite plate at the contact area in single lap, mechanically fastened joints. The analyses involve three dimensional finite element models performed by ABAQUS 6.4-PR11 code to evaluate the stress distribution in contact surface, separation angle, the magnitude and location of maximum radial stress. Results are determined for composite laminates with different layer configurations and attempts are made to validate the models with previous works. For cross ply and angle ply configurations only symmetric stacking sequences are used while for quasi-isotropic laminate both symmetric and non-symmetric models are generated. In cross-ply laminate symmetric separation about bearing plane could be found while in quasi-isotropic and angle-ply laminates non-symmetric separation occurs. Also, the separation angle is less than 90° in symmetric laminates and greater than 90° in some plies of non-symmetric laminates.

Key words: Finite element method, stress analysis, separation angle, single-lap mechanical joint

INTRODUCTION

In practical structures, composite laminates are often fastened to other structural components and a mechanical joint by means of pin or bolt is widely used. High stress concentration near the contact area between plates and pin may cause failure. As a result, composite bolted joints could fail at much lower bearing stress than their counterparts made of isotropic materials such as metals. The bearing stress is defined as the compressive load applied onto the laminate divided by the projected cross sectional area of the bearing surface. The projected area is calculated as the product of the diameter of the hole and the thickness of the laminate. Therefore, exact stress field is first step to get true outputs.

Analytical method is done by Madenci and Ileri (1993) to predict contact stresses in mechanical joints with single fastener, with two fasteners and with a row of fasteners. Experimental results are a large part of literature published and effects of clearance (Kelly and Hallström, 2004) and geometry parameters (İçten and Sayman, 2003; Okutan, 2002; Karakuzu *et al*., 2006; Mevlüt Tercan and Aktas, 2005) are investigated. Also, numerical models are generated and results are investigated. Okutan and Karakuzu (2003) investigate the effects of geometric dimensions on the strength of pinned joints and show a definite dependence of bearing strength on stacking sequence. Two different symmetric carbon-epoxy composite laminates are used to obtain the strength behavior and the optimum geometry of pinned joints using experimental and numerical models by Aktas and Dirikolu (2003, 2004). Three dimensional finite element analysis is used to examine the effects of bolt-hole clearance on behavior of composite bolted joints by McCarthy and McCarthy (2005).

In present study a three dimensional finite element model has been generated to solve for contact area in composite joints. As previously concluded, contact area is less than 180° (Chang, 1986) and its magnitude depends on geometry parameters, layer configurations, material properties and also friction and clearance between pin and plate. First, symmetric laminated composite models of quasi-isotropic, cross-ply and angle-ply configurations are generated to study the separation angle, the magnitude and location of maximum radial stress in each ply. Then, non-symmetric quasi-isotropic laminate is used to evaluate the behavior of laminated composite plate at contact surface. No previous three-dimensional studies on variation of separation angle through thickness and radial stress distribution in non-symmetric laminated joints have been found in literature.

PROBLEM DESCRIPTION

Consider a composite rectangular plate of length L, width W and thickness t with a hole of diameter D. The hole is at distance E from the free edge of the plate. This

Corresponding Author: V. Yavari, Department of Mechanical Engineering, Shiraz University, Shiraz, Iran
Tel: +98 917 311 9532 Fax: +98 711 626 3985

Table 1: The geometry parameters of the model

Length (L) (mm)	Width (W) (mm)	End distance (E) (mm)	Diameter (D) (mm)	Thickness (t) (mm)
280	32	32	6.822	1.61

Table 2: Elastic properties for the unidirectional lamina (Truong *et al*., 2002)

E_{11} (Gpa)	E_{22} (Gpa)	E_{33} (Gpa)	G_{12} (Gpa)	G_{13} (Gpa)	G_{23} (Gpa)	ν_{12}	ν_{13}	ν_{23}
98	7.8	7.8	4.7	4.7	3.2	0.34	0.34	0.44

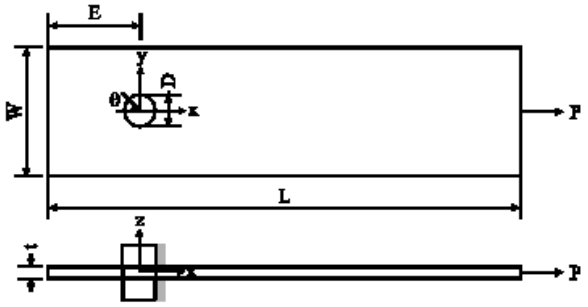

Fig. 1: The geometry of the pinned-joint problem

geometry is used with single pin to form a single lap joint (Fig. 1) and geometry parameters are shown in Table 1. The rigid pin is located at the center of the hole and a tensile load of 1.2 kN is applied to the plate. The laminated composite plate is consisted of eight layers with properties as in Table 2. Plate's layer configuration is changed to investigate the effects of that on the contact area. Only the case of equal pin and hole radius is investigated because it is sufficient for present purposes.

FINITE ELEMENT MODEL

The finite element method is used to determine the stress field around a hole in a pin-loaded laminate. The stress field around a hole in a laminate when subject to pin or bolt loading has been shown to be three-dimensional (Camanho *et al*., 1998; Ireman, 1998) and thus a three-dimensional finite element model is necessary to compute the multi-axial stress state which exists at the hole and the surrounding area. Finite element models of the pin-loaded laminates are developed using the ABAQUS (2001) finite element code (Fig. 2).

Each ply is modeled using a layer of linear isoparametric three-dimensional solid brick elements (C8D3), with the mesh being refined around the region adjacent to the hole in order to compute the contact stresses precisely (Fig. 3). Elements further afield from the hole where the aspect ratio of the elements was poorer are modeled using the reduced integration element (C8D3R) as reduced integration scheme alleviates the over-stiffened behavior of such elements.

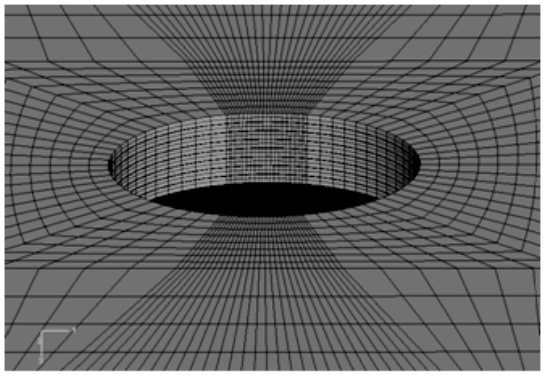

Fig. 2: The finite element mesh representing of the plate

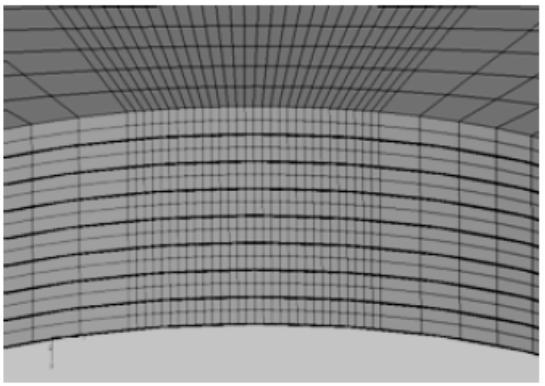

Fig. 3: Refined mesh around the hole at $\theta = \pm 90°$

The contact stress distribution and the full three-dimensional contact problem is solved in order to determine the actual contact pressure distribution and contact area. The master-slave contact algorithm is used based on finite sliding conditions (ABAQUS, 2001). The pin is modeled using an analytical rigid surface based on the work of Eriksson (1986) and Hyer *et al*. (1987) who concluded that the effect of pin modulus of elasticity is minor on the resulting contact stress distribution in the laminate. The use of an analytical contact surface is more computationally efficient and limits geometric discretisation error in comparison to modeling the pin using solid finite elements.

A frictionless contact is assumed between the pin and the plate. Geometrically linear analysis is performed as both the pin and the laminate are stiff bodies which do not undergo large rotations.

To assess the accuracy of the present finite element calculation, the distributions of the strain are verified by comparing results with those of previous work

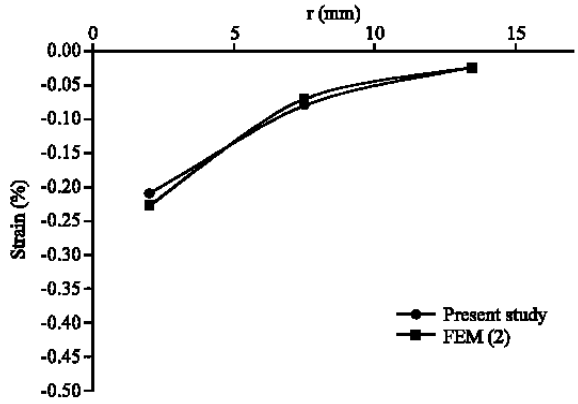

Fig. 4: Comparison of present results with previous results

as shown in Fig. 4 (Kelly and Hallström, 2004). Good accuracy could be found between the results.

SEPARATION ANGLES AND STRESS DISTRIBUTIONS IN CONTACT AREA FOR DIFFERENT CONFIGURATIONS

Tensile load, P and existence of interaction between the pin and the plate cause the deformation in the composite plate (Fig. 5). As a result of deformation, two separation locations occur at both sides of the pin and they are assumed to be constant through the thickness of the laminate in previous publications. In this study, analysis of the problem for different stacking sequences and various conditions is presented and in each section, reasons and explanations for the results have been given.

Symmetric laminated composite models of quasi-isotropic, cross-ply and angle-ply configurations are generated first to study the separation angle, the magnitude and location of maximum radial stress in each ply. Then, non-symmetric quasi-isotropic laminate is used to study the behavior of laminated composite plate at contact area. The stresses at the center of each ply are plotted. For better presentation of the figures, stresses are normalized by the average bearing stress. The average bearing stress is defined as:

$$\sigma_b = P/Dt. \quad (1)$$

Where:

P = The load
D = The hole diameter
t = The laminate thickness

Also θ_{max} and θ_s are the notations used to present maximum radial stress and separation locations.

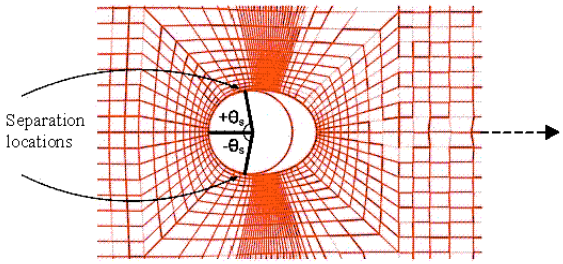

Fig. 5: Separation locations around the hole

Table 3: The magnitude and location of maximum radial stress and separation angle in each ply in symmetric quasi-isotropic $[0/45/90/-45]_s$ laminate

Ply No.	1 (0°)	2 (45°)	3 (90°)	4 (-45°)
$\sigma_{r\,max}$ (Mpa)	313	296	151	273
θ_{max} (degree)	0°	-40°	75°	40°
$-\theta_s$ (degree)	-84°	-83°	-87°	-80°
$+\theta_s$ (degree)	84°	81°	87°	83°

Symmetric quasi-isotropic laminate $[0/+45/90/-45]_s$: Radial stresses in each ply at the contact area are shown in Fig. 6. Because the stacking sequence is symmetric, results are only for four layers. The radial stresses are compressive regardless of ply orientation. Due to high stiffness in the loading direction, the 0° plies are under the highest stress. High radial stress levels are also evident in the ±45° plies with the peak load occurring close to the respective ply fiber directions where the stiffness is high. The radial stress distribution in these plies is non-symmetric about the bearing plane and the stresses in +45° plies are slightly higher than the -45° plies. The maximum radial stress in the 90° plies is shown to occur at $\theta_{max} = 75°$. The radial stress in 90° plies is significantly lower than the stresses in 0° and ±45° plies which is physically reasonable because the effective stiffness in the load direction is lower in 90° plies.

For better understanding, the maximum radial stresses, their locations (θ_{max}) and separation angle (θ_s) in each ply are shown in Table 3. The maximum radial stress is 313 Mpa and occurs in ply 1 (0°) at $\theta_{max} = \theta°$ which corresponds to the direction of applied load. High radial stresses also occur in ±45° plies (296 Mpa +45° plies and 273 Mpa in -45° plies). Due to the plies direction, maximum radial stresses in plies 2 and 4 (+45° and -45°) are lower than the maximum stress in ply 1 (0°). The maximum radial stress in ply 2 (+45°) is about 8% higher than the maximum stress in ply 4 (-45° ply). The radial stress in ply 3 (90°) is the lowest stress (151 Mpa) between plies which is physically reasonable with respect to fibers orientation. As it can be seen, in ply 1 (0°) and ply 3 (90°), the separation angles (θ_s) are symmetric (±84° and ±87°) while

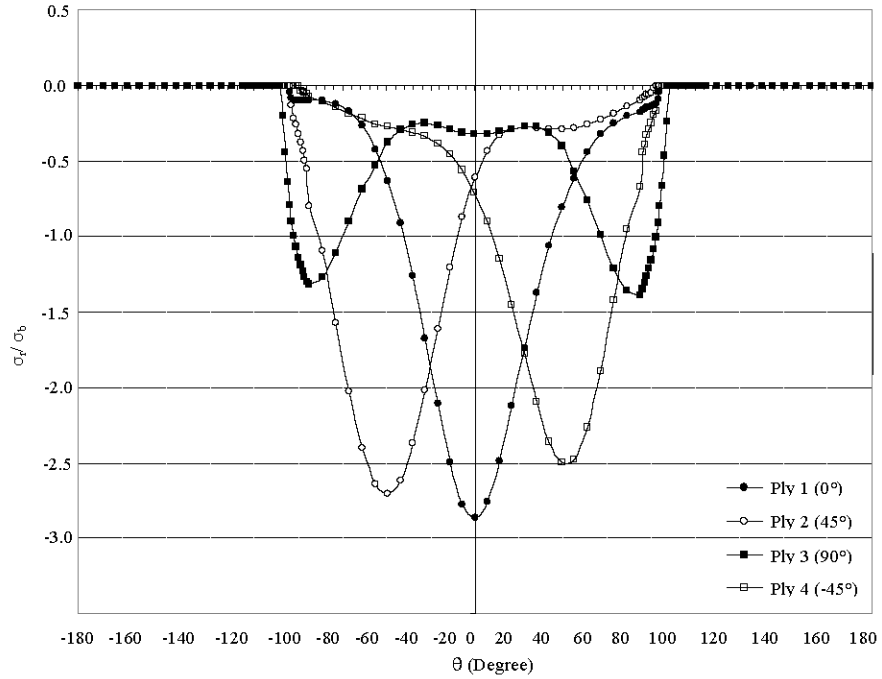

Fig. 6: Radial stress distribution around the hole in symmetric quasi-isotropic $[0/45/90/-45]_s$ laminate

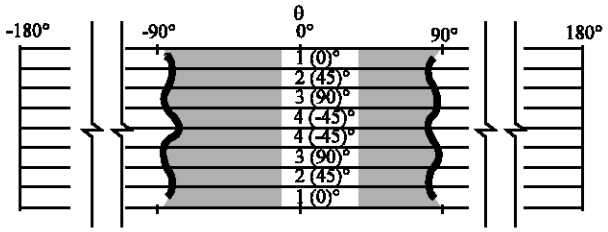

Fig. 7: Separation location in quasi-isotropic $[0/45/90/-45]_s$ laminate shown by (━━)

Table 4: The magnitude and location of maximum radial stress and separation angle in each ply in cross ply $[0_2/90_2]_s$ laminate

Ply No.	1 (0°)	2 (0°)	3 (90°)	4 (90°)
$\sigma_{r\,max}$ (Mpa)	231	252	130	106
θ_{max} (degree)	0°	0°	±60°	±63°
$-\theta_s$ (degree)	-80°	-80°	-81°	-80°
$+\theta_s$ (degree)	80°	80°	81°	80°

in ply 2 (45°) and ply 4 (-45°), the separation angles (θ_s) are non-symmetric (-83°, 81 and -80°, 83°). Due to stiffness, for ply 2 (45°) the magnitude of separation angle (θ_s) at clockwise direction is lower than the magnitude of separation angle (θ_s) in counterclockwise direction with respect to bearing plane while for ply 4 (-45°) is vise versa (Fig. 7).

Cross ply laminate $[0_2/90_2]_s$: The radial stress distribution for the cross ply laminate is shown in Fig. 8. Because the stacking sequence is symmetric, results are for only four layers. As can be seen, all the 0° plies have the maximum stresses at θ_{max} = 0°. The 90° plies experience their maximum stresses at an angle close to θ_{max} = 60°. The location of maximum radial stress θ_{max} is symmetric with respect to bearing plane as a result of symmetric stacking sequences. The magnitude and location of maximum radial stress θ_{max} and separation angle (θ_s) are shown in Table 4.

Due to cross-ply configuration, the separation angle (θ_s) is nearly constant through thickness. The separation angle (θ_s) is about 80° in all plies at both sides of contact area which is due to laminate stacking sequence (Fig. 9).

Angle ply laminate $[+45/-45]_{2s}$: The radial stresses distributions for the angle ply laminate are shown in Fig. 10. As can be seen, peak stresses occur close to ±34°. As a result of plies orientations, the location of maximum radial stress θ_{max} is non-symmetric with respect to bearing

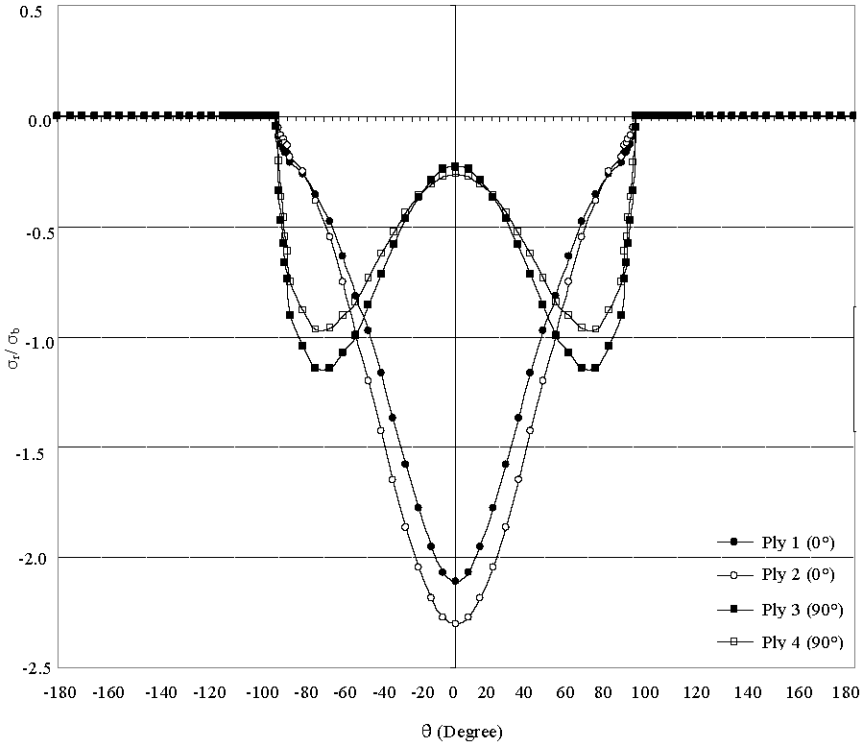

Fig. 8: Radial stress distribution around the hole in cross ply $[0_2/90_2]_s$ laminate

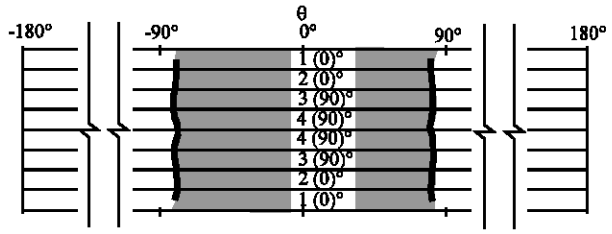

Fig. 9: Separation location in cross ply $[0_2/90_2]_s$ laminate shown by (⟶)

plane (Table 5, Fig. 11). The highest radial stress occurs in plies 2 (-45°) and 3 (45°).

Due to cross ply configuration, the separation angle (θ_s) is about 85° and nearly constant in all plies at both sides of contact area. The contact area through thickness is plotted in Fig. 11.

Non-symmetric quasi-isotropic laminate $[0_2/+45_2/90_2/(-45)_2]$: We shall now solve the problem for the non-symmetric quasi-isotropic laminate. The deformed shape of the joint model is shown with actual deformation in Fig. 12. More attention should be paid to this case for studying the results, because bending moment occurs in the laminate. Thus, as can be seen, results show a curvature in the laminated composite plate and the separation angles and contact area change sharply through the thickness of laminate. This is caused by the non-symmetry of the stacking sequence.

Table 5: The magnitude and location of maximum radial stress and separation angle in each ply in angle ply $[+45/-45]_{2s}$ laminate

Ply No.	1 (45°)	2 (-45°)	3 (45°)	4 (-45°)
$\sigma_{r\,max}$ (Mpa)	192	208	208	191
θ_{max} (degree)	-37°	34°	-34°	37°
$-\theta_s$ (degree)	-86°	-86°	-85°	-85°
$+\theta_s$ (degree)	85°	85°	85°	85°

Radial stresses in each ply at the contact area are shown in Fig. 13. Because the stacking sequence is non-symmetric, results are shown for all layers. Due to high stiffness in the loading direction, the 0° plies are under the highest stress. High radial stress levels are evident in the +45° plies too with the maximum load occurring close to

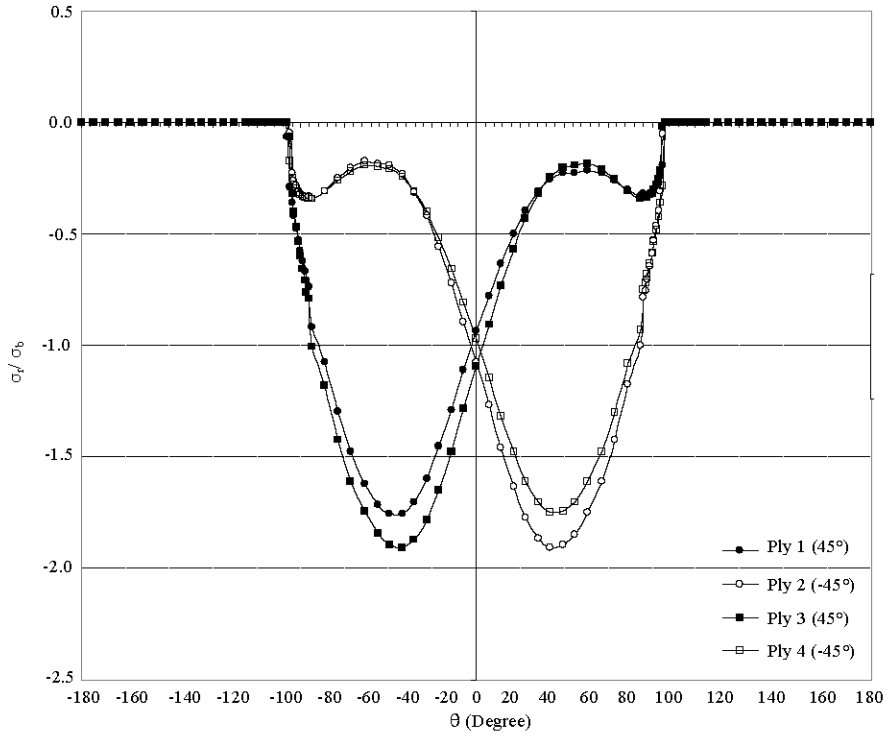

Fig. 10: Stress distribution around the hole in angle ply $[+45/-45]_{2s}$ laminate

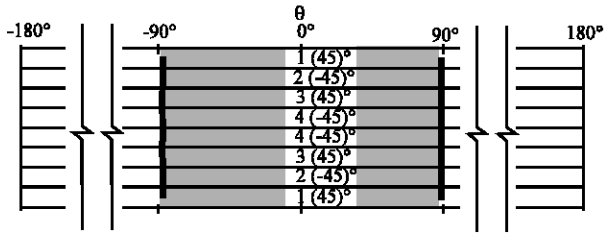

Fig. 11: Separation location in angle ply $[+45/-45]_{2s}$ laminate shown by (▬)

Fig. 12: Deformed shape of non-symmetric quasi-isotropic $[0_2/+45_2/90_2/(-45)_2]$ laminate

Table 6: The magnitude and location of maximum radial stress and separation angle in each ply in non-symmetric quasi-isotropic $[0_2/+45_2/90_2/(-45)_2]$ laminate

Ply No.	1 (0°)	2 (0°)	3 (45°)	4 (45°)	5 (90°)	6 (90°)	7 (-45°)	8 (-45°)
$\sigma_{r\,max}$ (Mpa)	458	450	336	305	170	147	187	83.7
θ_{max} (degree)	0	0	-34	-39	76	-76	45	51.0
$-\theta_s$ (degree)	-51	-57	-69	-69	-79	-88	-90	-99.0
$+\theta_s$ (degree)	93	91	89	86	89	86	79	76.0

the respective ply fiber directions. Stresses are also high in ply 7 (-45°) but extremely decrease in ply 8 (-45°). This could be reasonable because of the bending moment and curvature produced in laminated composite plate. The maximum radial stresses in 90° plies occur at $\theta_{max} = \pm 76°$.

For better understanding, the maximum radial stresses, their locations (θ_{max}) and separation angle (θ_s) in each ply are shown in Table 6. The maximum radial stress is 458 Mpa and occurs in ply 1 (0°) at $\theta_{max} = 0°$ which corresponds to the direction of applied load. High radial

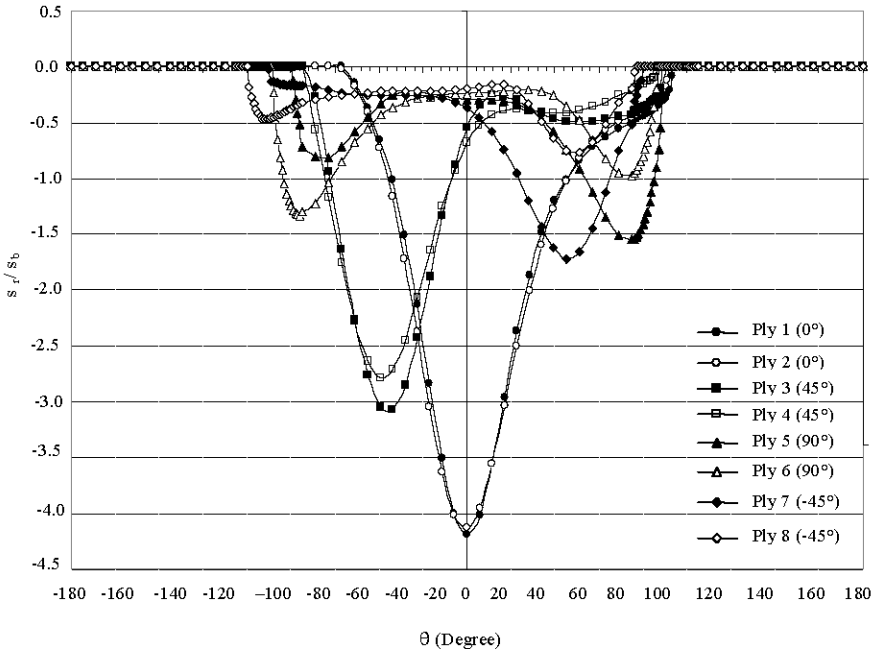

Fig. 13: Radial stress distribution around the hole in non-symmetric quasi-isotropic $[0_2/+45_2/90_2/(-45)_2]$ laminate

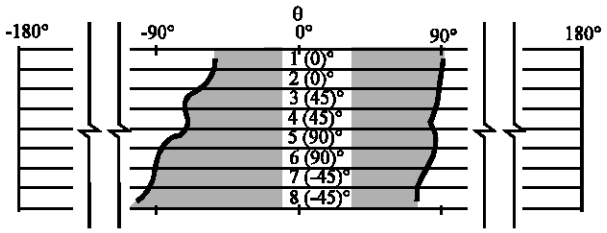

Fig. 14: Separation location in non-symmetric quasi-isotropic ply $[0_2/+45_2/90_2/(-45)_2]$ laminate shown by (▬▬)

stresses also occur in +45° plies (336 Mpa in ply 3 and 305 Mpa in ply 4). The radial stress in ply 8 (-45°) is the lowest stress (83.7 Mpa) between plies which is physically reasonable with respect to fibers orientation and laminated composite plate curvature. As it can be seen, the separation angles (θ_s) are non-symmetric with respect to bearing plane in all plies. It should be noted that separation angle (θ_s) magnitude is greater then 90° in ply 1 (0°), ply 2 (0°) and ply 8 (-45°) as a result of plate curvature (Fig. 14).

CONCLUSION

In this study, three-dimensional finite element analysis was used to examine the effects of layer configuration on the contact area of single-lap laminated composite pinned-joints. No previous three-dimensional study on variation of the contact area in symmetric and non-symmetric laminates through thickness has been found in the literature. The main findings from the study are summarized below.

In single-lap joints, the stress distribution in the laminate is non-uniform through the thickness and stacking sequence causes three-dimensional variation in this stress distribution.

Stress field is different in composite laminates with different stacking sequences. The minimum magnitudes of stresses occur in the angle-ply laminate, because none of the layers is oriented in the loading direction. Also because all layers are oriented at the same angle with respect to the loading direction, the magnitude of maximum stress does not differ significantly in the layers. Magnitudes of stress are larger in the cross ply laminate than the angle ply laminate and in the quasi-isotropic laminate are larger than the cross ply laminate. The cross ply laminate has four 0° plies which have more stiffness

with respect to 90° plies in the loading direction and stresses are divided between these 0° plies. This causes that the maximum radial stress in symmetric laminates occurs in the quasi-isotropic laminate which only has two 0° plies.

Results show the variation of the contact area through the thickness of the laminate even with symmetric stacking sequence. These variations are not investigated in previous works available in literature. So, this paper states why the contact problem of laminated composite joints should be solved in three dimensions.

In symmetric stacking sequences, the contact area is symmetric in 0° and 90° plies while it is non-symmetric in plies with other fiber orientations. Also, the contact area is less than 180°. In non-symmetric laminates, results show a curvature in the laminated composite plate and the separation angles and contact area change sharply through the thickness of laminate. Note that, the separation angle is greater than 90° in 0° and -45° plies but the contact area is less than 180° in all plies.

REFERENCES

ABAQUS Standard User's Manuals, 2001. Hibbet, Karlsson and Sorensen Inc., V6.4-PR11. Pawtucket, RI, USA.

Aktas, A. and H.M. Dirikolu, 2003. The effect of stacking sequence of carbon epoxy composite laminates on pinned-joint strength. Composite Struct., 62: 107-111.

Aktas, A. and H.M. Dirikolu, 2004. An experimental and numerical investigation of strength characteristics of carbon-epoxy pinned-joint plates. Composites Sci. Technol., 64: 1605-1611.

Camanho, P.P., S. Bowron and F.L. Matthews, 1998. Failure mechanisms in bolted CFRP. J. Reinforced Plastics Composites, 17: 205-233.

Chang, F.K., 1986. The effect of pin load distribution on the strength of pin loaded holes in laminated composites. J. Composite Mater., 20: 401-408.

Eriksson, L.I., 1986. Contact stresses in bolted joints of composite laminates. Composite Struct., 6: 57-75.

Hyer M.W., E.C. Klang and D.E. Cooper, 1987. The effects of pin elasticity, clearance and friction on the stresses in a pin-loaded orthotropic plate. J. Composite Mater., 21: 190-206.

İçten, B.M. and O. Sayman, 2003. Failure analysis of pin-loaded aluminum-glass-epoxy sandwich composite plates. Composites Sci. Technol., 63: 727-737.

Ireman, T., 1998. Three-dimensional stress analysis of bolted single-lap joints. Composite Struct., 43: 195-216.

Karakuzu, R., T. Gülem and B.M. İçten, 2006. Failure analysis of woven laminated glass-vinylester composites with pin-loaded hole. Composite Struct., 72: 27-32.

Kelly, G. and S. Hallström, 2004. Bearing strength of carbon fibre/epoxy laminates: Effects of bolt hole clearance. Composites, Part B, 35: 331-343.

Madenci, E. and L. Ileri, 1993. Analytical determination of contact stresses in mechanically fastened composite laminates with finite boundaries. Int. J. Solids Struct., 30: 2469-2484.

McCarthy, C.T. and M.A. McCarthy, 2005. Three-dimensional finite element analysis of single-bolt, single-lap composite bolted joints: Part II-effects of bolt-hole clearance. Composite Struct., 71: 159-175.

Mevlüt Tercan, O.A. and A. Aktaş, 2005. An experimental investigation of the bearing strength of weft-knitted 1×1 rib glass fiber composites. Composite Structures, November 2005.

Okutan, B., 2002. The effects of geometric parameters on the failure strength for pin-loaded multi-directional fiber-glass reinforced epoxy laminate. Composites, Part B, 33: 567-578.

Okutan, B. and R. Karakuzu, 2003. The strength of pinned joints in laminated composites. Composites Sci. Technol., 63: 893-905.

Truong Chi, T., S.V. Lomov and I. Verpoest, 2002. The mechanical properties of multi-axial multi-ply carbon fabric reinforced epoxy composites. Proceedings of the 10th European Conference on Composite Materials (ECCM-10), Brugge, Belgium.